The British Journal of Radiology, 83 (2010), 218–224

Sphenoid sinus ectopic pituitary adenomas: CT and MRI findings

[1]B T YANG, MD, [2]V F H CHONG, MD, [1]Z C WANG, MD, [1]J F XIAN, MD and [1]Q H CHEN, MD

[1]*Department of Radiology, Beijing Tongren Hospital, Capital Medical University, Beijing, China, and* [2]*Department of Diagnostic Radiology, National University Hospital and Yong Loo Lin School of Medicine, National University of Singapore, Singapore*

ABSTRACT. Ectopic pituitary adenomas (EPAs) are rare lesions. The purpose of this study was to describe the CT and MRI features of sphenoid sinus EPAs. Eight patients with histology-proven EPAs in the sphenoid sinus, all of whom underwent CT and MRI, were reviewed retrospectively. The following imaging features were analysed: (i) size, (ii) margin, (iii) CT attenuation characteristics and (iv) MRI signal intensity. In addition, the involvement of adjacent structures and the time–intensity curve (TIC) of dynamic contrast-enhanced (DCE) MRI were analysed. All EPAs had well-defined margins and showed no relationship to the intrasellar pituitary gland. The mean size was 28 mm (range, 20–46 mm). On non-enhanced CT, the lesions appeared isodense to grey matter in 7 (88%) patients and hypodense in 1 (12%) patient. Only two patients underwent post-contrast CT, and they showed moderate enhancement. On T_1 weighted images, EPAs appeared isointense in 6 (75%) patients and hypointense in 2 (25%). On T_2 weighted images, the lesions appeared hyperintense in 2 (25%) patients and isointense in 6 (75%). EPAs showed mild to moderate heterogeneous contrast enhancement and exhibited a cribriform-like appearance. Two patients underwent DCE MRI; the TIC showed a rapidly enhancing and slow washout pattern. The following features were also seen: an empty sella, bone changes and involvement of the cavernous sinus (5 patients; 62.5%). In conclusion, a high index of suspicion for EPA and a familiarity with the imaging findings may help to diagnose this rare entity accurately.

Received 14 December 2008
Revised 3 March 2009
Accepted 27 March 2009

DOI: 10.1259/bjr/76663418

Sphenoid sinus ectopic pituitary adenomas (EPAs) are extremely rare, and most of the papers in the literature are case reports. A review of the English literature has shown, to date, fewer than 40 cases [1–6]. Furthermore, some authors think a pre-operative diagnosis of EPA is often difficult to make. We reviewed retrospectively the CT and MRI findings of eight patients with histology-proven EPAs in the sphenoid sinus. The findings in this paper may help to increase the awareness of this entity among both clinicians and radiologists. An accurate diagnosis of EPA will help to formulate the most appropriate management approach.

Methods and materials

Patients

This study was approved by the institutional review board. A retrospective review of 249 image-detected sphenoid sinus lesions over a six-year period (August 2002 to April 2008) revealed eight (3%) patients with histology-proven EPAs, comprising three (37.5%) males and five (62.5%) females. The average age was 58 years (range, 41–70 years). All eight patients underwent surgical removal of EPAs by endoscopic sinus surgery (ESS). The clinical presentations, histological diagnosis and hormonal levels were extracted from the medical records.

Address correspondence to: Ben Tao Yang, Department of Radiology, Beijing Tongren Hospital, Capital Medical University, No.1, Dongjiaominxiang, Dongcheng District, Beijing 100730, China. E-mail: cjr.yangbentao@vip.163.com

CT technique

All eight patients initially presented to the otolaryngology clinic with nasal presentations and underwent paranasal sinus CT. Images were acquired in both the axial and coronal planes in seven patients, and in the coronal plane only in one patient using a GE Sytec 4000i (General Electric Company, USA), Siemens Somatom Plus 4 (Siemens Company Berlin, Germany) or GE HiSpeed NX/i CT system (General Electric, USA). The imaging parameters were: voltage 120 kV, current 200 mA, matrix 512 × 512 and section thickness 2 mm. Examinations were performed from the anterior wall of the frontal sinus to the posterior wall of the sphenoid sinus. Images were reconstructed using both a bone algorithm (window width of 1500 Hounsfield units (HU) or 2000 HU at a window level of 150 HU or 200 HU) and a soft-tissue algorithm (window width of 400 HU at a window level of 40 HU). Two patients underwent contrast-enhanced CT studies (100 ml of Omnipaque at 300 mg I ml^{-1} injected at 2.5 ml s^{-1}; GE Healthcare, China).

MRI technique

All eight patients underwent sphenoid sinus MRI before ESS. The MR examinations were performed on a 1.5 T unit

MR system (GE Signa, USA) with a head coil. Fast spin-echo pulse sequences were used in these patients. All eight patients underwent pre-enhanced (T_1 weighted imaging (T1WI) and T_2 weighted imaging (T2WI)) and post-enhanced (T1WI) in the axial, coronal and sagittal planes. The imaging parameters were as follows. T1WI: repetition time (TR) 500–600 ms, echo time (TE) 10–15 ms; T2WI: TR 3000–3500 ms, TE 120–130 ms; excitations 2–4; echo train length 11–27; matrix 256 × 256; field of view (FOV) 20 × 20 cm; section thickness 4–5 mm; intersection gap 0.0–0.5 mm.

Post-contrast T_1 weighted images with frequency-selective fat saturation were acquired in the optimal plane after dynamic contrast-enhanced (DCE) MRI. Rapid manual bolus intravenous injection (2 ml s^{-1}) of 0.1 mmol gadopentetate dimeglumine (Magnevist; Schering, Germany) per kilogram of body weight was followed by a 10 ml flush of normal saline solution. DCE MRI was performed by using three-dimensional fast spoiled gradient echo before conventional post-contrast T1WI in two patients. The following scan parameters were used: TR 8.4 ms; TE 4.0 ms; excitation 1; matrix 256 × 160; FOV 20 × 20 cm; section thickness 3.2 mm; and intersection gap 0 mm. A total of 12 sets of dynamic images were obtained. Each set included six images and took 13 s; the inter-set time gap was 12 s. The whole dynamic series took 5 min in total. After the dynamic scan, source images were transferred to an imaging workstation for further analysis. In the maximal section of the tumours, the authors manually drew regions of interest (ROIs) for signal intensity measurements to avoid cystic and necrotic areas. ROIs were approximately 3–4 mm in diameter. In order to ensure the accuracy of the time–intensity curve (TIC), several ROIs were chosen on the basis of lesion size and subsequently compared with the histopathology. Concurrently, the change in signal intensity of a similar ROI placed on the masticator muscle was used for reference.

Image analysis

The CT and MR images were evaluated by three experienced radiologists, and the findings were reached by consensus.

In the present study, we used the classification of the TIC of DCE MRI proposed by Yabuuchi et al [7]:

- Type I (steady enhancement pattern) appears as a straight or curved line; enhancement continues over the entire dynamic study.
- Type II (rapidly enhancing and slow washout pattern) appears as growing enhancement at an early stage and then displays a sharp bend to form a plateau at the middle and later stages.
- Type III (rapidly enhancing and rapid washout pattern) appears as growing enhancement during the early stage and then progressively decreases in signal intensity.

Results

The most common symptoms of the patients were nasal obstruction (8/8; 100%), rhinorrhoea (4/8; 50%), headache (4/8; 50%), epistaxis (2/8; 25%), dysosmia (2/8; 25%) and decrease in vision (2/8; 25%). Of the four patients with rhinorrhoea, one had cerebrospinal fluid leakage. Table 1 summarises the main clinical manifestations, histological diagnoses and hormonal statuses.

In this series, half of the patients had hormone-secreting adenoma (three prolactinomas and one adrenocorticotropic hormone (ACTH)-secreting adenoma). Two male patients with prolactinoma had a 3- to 4-year history of impotency and testicular atrophy. The female patient with prolactinoma also had amenorrhoea of approximately 30 years' duration. The patient with

Table 1. Sphenoid sinus ectopic pituitary adenomas: symptoms, histological diagnosis and hormonal status

Patient no.	Sex	Age (years)	Primary symptoms	Histopathology	Hormonal status
1	F	66	Nasal obstruction, rhinorrhoea, headache, amenorrhoea	Prolactinoma	PRL >80 ng ml^{-1} (normal range, 2.64–13.13 ng ml^{-1}); GH 0.139 μg l^{-1} (normal range, 1–10 μg l^{-1})
2	F	61	Nasal obstruction, epistaxis, Cushing's symdome	ACTH-secreting adenoma	60 pg ml^{-1} (normal range, 0–46 pg ml^{-1})
3	M	57	Nasal obstruction, rhinorrhoea, headache, impotency	Prolactinoma	PRL >200 ng ml^{-1} (normal range, 2.64–13.13 ng ml^{-1}); testosterone 0.97 ng ml^{-1} (2.8–8 ng ml^{-1})
4	M	41	Nasal obstruction, epistaxis, impotency	Prolactinoma	PRL 17680 μIU ml^{-1} (normal range, 98–456 μIU ml^{-1}); testosterone 0.76 ng ml^{-1} (2.8–8 ng ml^{-1})
5	M	60	Nasal obstruction, headache	Non-functioning adenoma	Non-secreting
6	F	64	Nasal obstruction, rhinorrhoea, visual decrease	Non-functioning adenoma	Non-secreting
7	F	45	Nasal obstruction, rhinorrhoea, headache	Non-functioning adenoma	Non-secreting
8	F	70	Nasal obstruction, decreased visual acuity	Non-functioning adenoma	Non-secreting

M, male; F, female; ACTH, adrenocorticotropic hormone; PRL, prolactin; GH, growth hormone.

ACTH-secreting adenoma had the signs and symptoms of Cushing's disease.

In all imaging studies, sphenoid sinus EPAs showed no connection to the intrasellar pituitary gland (Figures 1a,c, 2c,d and 3a,b). This was confirmed at endoscopic surgery when the sellar dura was noted to be intact. The imaging characteristics are summarised in Table 2. All EPAs show well-defined margins. three lesions (37.5%) showed an ovoid configuration, whereas 5 (62.5%) lesions demonstrated a nondescript irregular shape. The mean maximum diameter was 28 mm (range, 20–46 mm).

On non-enhanced CT, the lesions appeared isodense to grey matter in seven patients (87.5%) and slightly hypodense in 1 (12.5%). Only two patients underwent post-contrast CT, and they showed relatively homogeneous moderate enhancement. In five (62.5%) patients, there was local bony displacement or erosion in the sellar floor.

On T1WI, EPAs appear isointense in six (75%) patients (Figures 1a and 3a,b) and slightly hypointense in two (25%). On T2WI, the lesions appear slightly hyperintense in two (25%) patients (Figures 2a and 3c) and isointense in six (75%) (Figure 1b). These lesions show a stippled low-signal-intensity appearance within the mass, giving rise to a cribriform pattern. These low-signal-intensity foci on T2WI showed correspondingly high signal intensity (Figure 2a). These features appear to be related to small fluid-filled spaces seen in histological observations.

Relatively large cystic foci in EPAs were noted in two (25%) patients, and the lesions showed low signal intensity on T1WI and high signal intensity on T2WI. In 1 (12.5%) patient, the cystic focus appears as high signal intensity on T1WI and relatively low signal intensity on T2WI (Figure 3). These signal changes reflect the proteinaceous nature of the secretions histologically.

EPAs typically show mild to moderate heterogeneous on conventional contrast-enhanced images and manifest as a characteristic cribriform-like appearance (Figures 1c and 2b). Two patients underwent DCE MRI; the TIC showed a rapidly enhancing and slow washout pattern. According to the classification proposed by Yabuuchi et al [7], the TICs of DCE MRI in our two patients were consistent with the Type II classification (Figure 2e,f).

The following features are also seen: (i) empty sella (5/8; 62.5%), (ii) bone changes (5/8; 62.5%) and (iii) involvement of cavernous sinus (5/8; 62.5%). An empty sella associated with sphenoid sinus EPA is most elegantly demonstrated on sagittal MRI (Figures 1c and 3b). The most common manifestation of bony involvement is a smooth remodelling (Figures 1b,c and 2a–c) or erosion of the clivus (Figure 3b,c). Tumour extension into the cavernous sinus, which encases the adjacent internal carotid artery, can occur (Figures 2a,d and 3a).

Discussion

EPAs are defined as extrasellar pituitary adenomas that show no connection to the normal pituitary gland. They usually occur along the cephalic migration pathway of Rathke's pouch. During the ingrowth of Rathke's pouch, pituitary tissues can be retained in the sphenoid sinus and remain separate from the normal pituitary gland [1–4, 6, 8]. The sphenoid sinus is the most common site for EPA, followed by the suprasellar region; other less common sites include the cavernous sinus, parasellar region, clivus, nasal cavity, nasopharynx, temporal bone and third ventricle [6]. Embryological rests may show hormonal activity, respond to change in endocrine feedback, and have the potential to develop adenomas [3, 4, 8].

Sphenoid sinus EPAs present most frequently in the fourth to seventh decades of life; the mean age at diagnosis is 51.4 years old [6]. Women are affected more than men [5, 6]. The various clinical presentations depend on the space-occupying effect of the lesion or hormonal activity. The primary clinical symptoms of sphenoid sinus EPA include nasal obstruction, headache, a decrease in vision and cerebrospinal fluid leak. 58% of patients show evidence of hyperfunctional hormonal activity, including Cushing's syndrome, acromegaly and hyperparathyroidism [9]. The hyperfunctioning adenoma was observed in 4 (50%) patients in the present series.

In the assessment of sphenoid sinus EPAs, CT and MRI are complementary. CT often provides important information regarding the bony anatomy of the paranasal sinus and skull base that helps in the planning of endoscopic surgery. On non-enhanced CT, EPAs are usually isodense in relation to grey matter and they rarely show calcification. They usually show moderate enhancement. Depending on the size of the lesions, they may cause adjacent bone remodelling, sclerosis or erosion. Involvement of adjacent bone was noted in 5 patients (62.5%) in this series and is therefore a common feature of sphenoid sinus EPAs.

MRI demonstrates clearly the relationship between EPAs and the normal location of the pituitary glands, the cavernous sinus and internal carotid arteries. Such information facilitates surgical planning. On MRI, lesions are usually isointense relative to adjacent grey matter, and they show mild to moderate enhancement after the administration of contrast material. They are usually heterogeneous, demonstrating foci of low signal intensity on T1WI and high signal intensity on T2WI. Histologically, these foci correspond to enlarged spaces filled with secretions. The solid areas of EPAs show strong enhancement and, when juxtaposed with the relatively low signal intensity of secretion-filled spaces, result in a characteristic cribriform pattern, which may be an important suggestive sign. Sphenoid sinus EPAs with relatively large cyst formation, necrosis, haemorrhage or proteinaceous secretions were reported to be seldom seen [1–4]. However, three cases with cysts were identified in the present series. Similar to pituitary adenomas, EPAs have a preferential growth pattern that involves the cavernous sinus and encases adjacent internal carotid arteries, which may act as a helpful sign for differentiating them from other tumours in the sphenoid sinus.

Sphenoid sinus EPAs may occur in association with empty sellas, which probably gives a diagnostic clue to this entity in this region, of which there have been six previous reports [1–4, 10, 11]. In our series, there were five (62.5%) patients with empty sellas. The association between EPAs and an empty sella is not clearly understood. It has been suggested that, during the formation of the anterior pituitary gland, most of the nasopharyngeal precursors (which later give rise to EPAs) remain in the sphenoid bone (which later become the sphenoid sinus). In these patients, only a small number of cells migrated to form the anterior pituitary, thus resulting in the

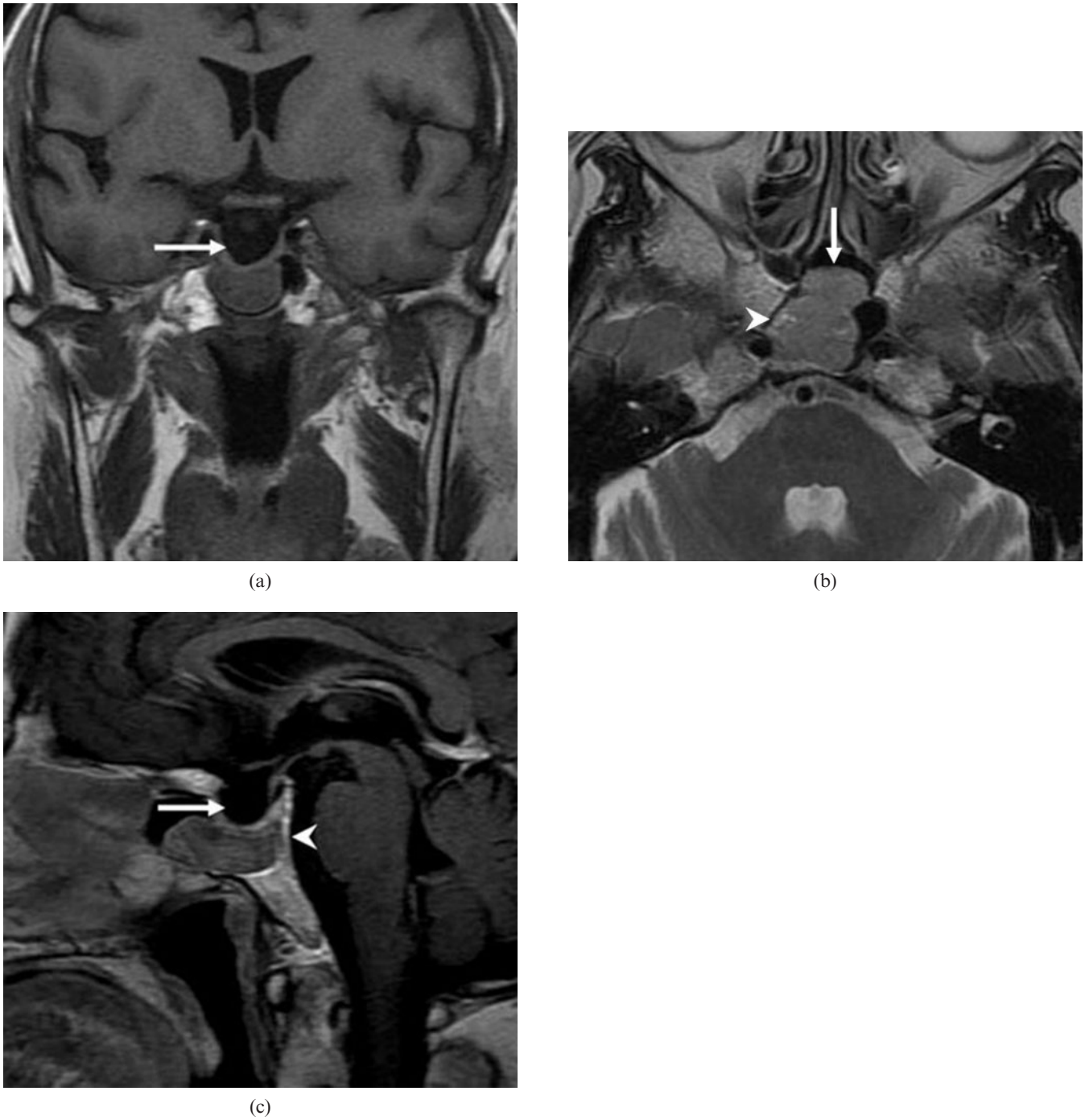

Figure 1. Patient 2. (a) Coronal T_1 weighted MR image shows a well-defined mass of isointense signal intensity in the sphenoid sinus with an intact sellar floor and empty sella (arrow). (b) Axial T_2 weighted MRI shows a mass of intermediate signal intensity (arrow) with small foci of high signal intensity (arrowhead). Note the tumour compressing the adjacent clivus. (c) Sagittal contrast-enhanced MRI shows a mass of well-defined moderate heterogeneous enhancement. There is a thin gap between the superior margin of the tumour and sellar floor. Note the intacting sellar floor, mild remodelling of the adjacent clivus (arrowhead) and empty sella (arrow).

formation of empty sellas [2, 10, 11]. Esteban et al [12] postulated that the empty sella in their patient was possibly secondary to radiation therapy for Cushing's syndrome. None of our patients had a history of irradiation, and the presence of empty sellas is likely to be related to anomalous development.

DCE MRI can provide information related to tumour perfusion, microvascular permeability and volume of the extracellular space, and such information may help to predict the histology of lesions [7]. For example, a TIC of DCE MRI may provide additional information to help differentiate benign from malignant lesions [7]. The TIC of our two patients showed Type II characteristics. To the best of our knowledge, there have been no previously documented reports on DCE MRI of sphenoid sinus EPAs. However, there are a few reports on the TIC of DCE MRI in pituitary adenomas, which also had Type II characteristics [13]. This technique may therefore serve

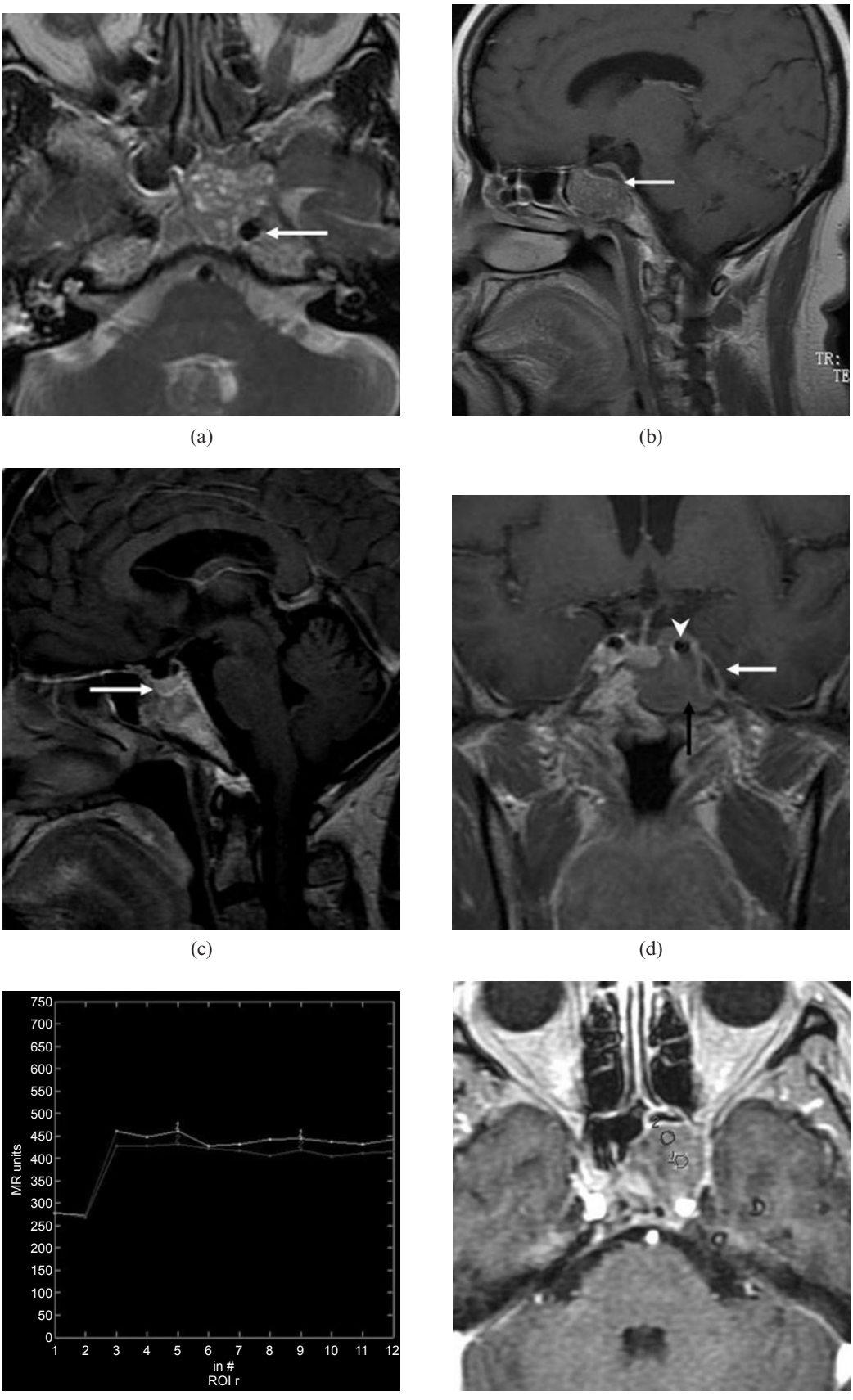

(a) (b) (c) (d) (e) (f)

Figure 2. (see next page for caption)

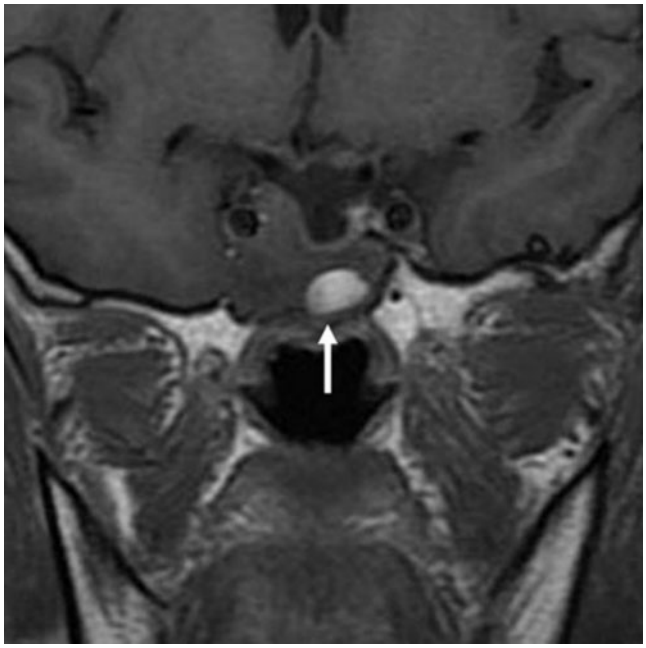

(a)

(b)

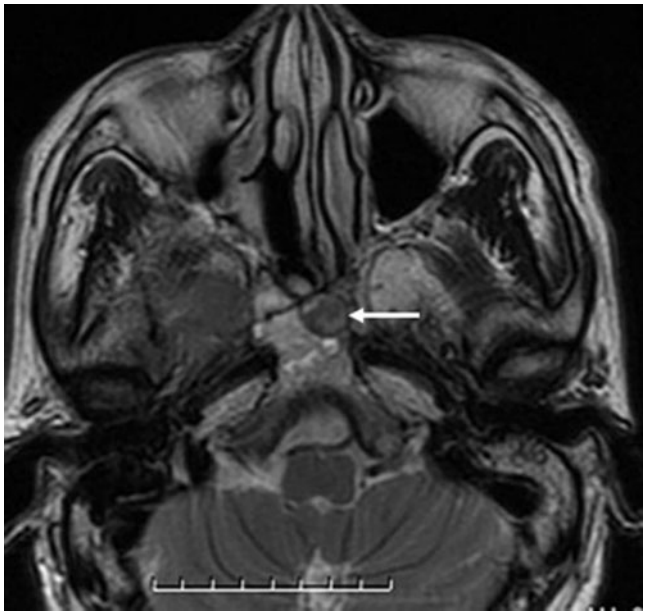

(c)

Figure 3. (above) Patient 5 (had right nasal cavity endoscopic sinus surgery owing to a papilloma 10 years ago). (a) Coronal T_1 weighted MR image shows heterogeneous sphenoid sinus ectopic pituitary adenoma with an area of high signal intensity (arrow), suggesting proteinaceous secretions. Note the presence of an empty sella and encasement of the right internal carotid artery. (b) Sagittal T_1 weighted MR image shows an empty sella and intact sellar floor (arrow). Note the erosion of the adjacent clivus. (c) Axial T_2 weighted MR image shows a sphenoid sinus mass of slightly high signal intensity with area of low signal intensity (arrow). Note the erosion of the adjacent clivus.

Figure 2. (previous page) Patient 1. (a) Axial T_2 weighted MR image shows a sphenoid sinus mass of slightly high signal intensity with multiple foci of high signal intensity in the cystic spaces. Note the encasement of the left internal carotid artery (arrow) and compression of the adjacent clivus. (b) Paramidline sagittal contrast-enhanced MR image shows mild heterogeneous tumour enhancement exhibiting a cribriform pattern. Note the mild remodelling of the clivus and continuity of the sellar floor (arrow). (c) Midline sagittal contrast-enhanced MR image shows an intact sellar floor (arrow). (d) Coronal contrast-enhanced MR image shows tumour in the left sphenoid sinus (black arrow) involving the left carotid artery (arrowhead) and left cavernous sinus (white arrow). Note the normal enhancing pituitary gland. (e) Corresponding axial dynamic contrast-enhanced MR image depicts the rapidly enhancing and slow washout pattern (Type 2). (f) The two round cursors mark the region of interest selected for signal intensity measurement on dynamic MRI.

Table 2. Sphenoid sinus ectopic pituitary adenomas: CT and MRI characteristics

Patient no.	Lesion size (mm)	CT		MRI		
		Pre-contrast	Contrast	T1WI	T2WI	Contrast
1	20	Isodense	–	Isointense	Slightly hyperintense	Mild
2	24	Isodense	–	Isointense	Isointense	Moderate
3	28	Isodense	Moderate	Isointense	Isointense	Moderate
4	22	Isodense	–	Slightly hypointense	Isointense	Moderate
5	23	Slightly hypodense	–	Isointense	Slightly hyperintense	Moderate
6	31	Isodense	Moderate	Slightly hypointense	Isointense	Moderate
7	30	Isodense	–	Isointense	Isointense	Mild
8	46	Isodense	–	Isointense	Isointense	Moderate

Lesion size indicates maximum diameter. CT density and MRI signal intensity are relative to cerebral grey matter. T1WI, T_1 weighted image; T2WI, T_2 weighted image.

as an additional method for predicting the nature of a suspected EPA in the sphenoid sinus.

Sphenoid sinus EPAs should be differentiated from other lesions in the central skull base. Chordomas are often destructive lesions, and CT often shows calcification, residual bone fragments and minimal enhancement. On MRI, chordomas typically show variable signal intensity on both T1WI and T2WI, and contrast enhancement is low. Cartilaginous lesions usually reveal calcifications. These lesions typically reveal peripheral and septal contrast enhancement [14]. Craniopharyngiomas generally have sellar and suprasellar components, and extracranial lesions confined to the sphenoid sinus are rare. On CT, fungus balls in the sphenoid sinus often demonstrate punctate or fine-linear patterns of radiodensities. On MRI, fungus balls characteristically reveal intermediate signal on T1WI and low signal intensity on T2WI and demonstrate no enhancement.

In conclusion, a diagnosis of sphenoid sinus EPA requires a strong index of suspicion. MRI findings, including an intact sellar floor, signal characteristics and association with an empty sella, are often suggestive of this entity. CT is complementary and provides useful information on paranasal sinus and skull base anatomy required for endoscopic surgery.

References

1. Slonim SM, Haykal HA, Cushing GW, Freiderg SR, Lee AK. MRI appearances of an ectopic pituitary adenoma: case report and review of the literature. Neuroradiology 1993;35:546–8,
2. Das CJ, Seith A, Gamanagatti S, Goswami R. Ectopic pituitary adenoma with an empty sella. AJR Am J Roentgenol 2006;186:1468–9.
3. Hattori N, Ishihara T, Saiwai S, Moridera K, Hino M, Ikekubo K, et al. Ectopic prolactinoma on MRI. J Comput Assist Tomogr 1994;18:936–8.
4. Gondim JA, Schops M, Ferreira E, Bulcao T, Mota JI, Silveira C. Acromegaly due to an ectopic pituitary adenoma in the sphenoid sinus. Acta Radiol 2004;45:689–91.
5. Suzuki J, Otsuka F, Ogura T, Kishiela M, Takeda M, Tamiya T, et al. An aberrant ACTH-producing ectopic pituitary adenoma in the sphenoid sinus. Endocr J 2004;51:97–103.
6. Hou L, Harshbarger T, Herrick MK, Tse V. Suprasellar hormone-secreting ectopic pituitary adenoma: case report and literature review. Neurosurgery 2002;50:618–25.
7. Yabuuchi H, Fukuya T, Tajima T, Hachitanela Y, Tomita K, Koga M. Salivary gland tumors: diagnostic value of gadolinium-enhanced dynamic MR imaging with histopathologic correlation. Radiology 2003;226:345–54.
8. Madonna D, Kendler A, Soliman AM. Ectopic growth hormone-secreting pituitary adenoma in the sphenoid sinus. Ann Otol Rhinol Laryngol 2001;110:99–101.
9. Langford L, Batsakis JG. Pituitary gland involvement of sinonasal tract. Ann Oto Rhinol Laryngol 1995;104:167–9.
10. Hori E, Akai T, Kurimoto M, Hirashima Y, Endo S. Growth hormone-secreting pituitary adenoma confined to the sphenoid sinus associated with a normal-sized empty sella. J Clin Neurosci 2002;9:196–9.
11. Matsuno A, Katayama H, Okazaki R, Toriumi M, Tanaka H, Akashi M, et al. Ectopic pituitary adenoma in the sphenoid sinus causing acromegaly associate with empty sella. ANZ J Surg 2001;71:495–8.
12. Esteban F, Ruiz-Avila I, Vilchez R, Gamero C, Gomez M, Mochon A. Ectopic pituitary adenoma in the sphenoid causing Nelson's syndrome. J Laryngol Otol 1997;111:565–7.
13. FitzPatrick M, Tartaglino LM, Hollander MD, Zimmerman RA, Flanders AE. Imaging of sellar and parasellar pathology. Radiol Clin North Am 1999;37:101–21.
14. Yang BT, Wang ZC, Liu S, Xian JF, Zhang ZY, Liu ZL, et al. CT and MRI diagnosis of chondrosarcoma in sinonasal and orbital region. Chinese J Radiol 2006;40:572–6.